Front. Phys. 11(2), 117801 (2016)
DOI 10.1007/s11467-016-0551-z

REVIEW ARTICLE

Graphene-plasmon polaritons: From fundamental properties to potential applications

Sanshui Xiao[1,2,*], **Xiaolong Zhu**[3], **Bo-Hong Li**[1,2], **N. Asger Mortensen**[1,2,†]

[1] *Department of Photonics Engineering, Technical University of Denmark, DK-2800 Kgs. Lyngby, Denmark*
[2] *Center for Nanostructured Graphene, Technical University of Denmark, DK-2800 Kgs. Lyngby, Denmark*
[3] *Department of Micro and Nanotechnology, Technical University of Denmark, DK-2800 Kgs. Lyngby, Denmark*

*Corresponding authors. E-mail: *saxi@fotonik.dtu.dk, †asger@mailaps.org*

Received December 29, 2015; accepted January 11, 2016

With unique possibilities for controlling light in nanoscale devices, graphene plasmonics has opened new perspectives to the nanophotonics community with potential applications in metamaterials, modulators, photodetectors, and sensors. In this paper, we briefly review the recent exciting progress in graphene plasmonics. We begin with a general description of the optical properties of graphene, particularly focusing on the dispersion of graphene-plasmon polaritons. The dispersion relation of graphene-plasmon polaritons of spatially extended graphene is expressed in terms of the local response limit with an intraband contribution. With this theoretical foundation of graphene-plasmon polaritons, we then discuss recent exciting progress, paying specific attention to the following topics: excitation of graphene plasmon polaritons, electron-phonon interactions in graphene on polar substrates, and tunable graphene plasmonics with applications in modulators and sensors. Finally, we address some of the apparent challenges and promising perspectives of graphene plasmonics.

Keywords graphene, plasmonics, graphene-plasmon polariton, plasmon-phonon interaction, tunability

PACS numbers 78.67.-n, 41.20.Jb, 42.25.Bs

Contents

1 Introduction

Plasmonics [1, 2], as a separate branch of nanophotonics, has recently attracted intensive attention driven by both emerging applications and maturing state-of-the-art nanofabrication technology [3–5]. With strong interaction between light and free electrons, plasmonics allows breaking the diffraction limit [6, 7] to concentrate light into deep-subwavelength volumes with huge field enhancements [1, 3, 8–10]. The fascinating properties of plasmonics provide a foundation for various applications, including integrated optical circuits [11–13], single-molecule detection [14, 15], super-resolution imaging [16, 17], photovoltaics [18, 19], color generation [20–22], and biological sensing [23, 24]. These achievements have mostly been realized in the visible or near-infrared regions where the noble metals host plasmons that can be driven by light fields.

With the rapid rise of the use of graphene, new scientific and technological opportunities are appearing [25]; in the context of optoelectronics and photonics, highly doped graphene is considered to be a promising plasmonic material working in the mid-infrared and terahertz (THz) spectral windows [26–30]. Compared to plasmon polaritons in noble metals [31], graphene-plasmon polaritons (GPPs) exhibit even stronger mode confinement and relatively longer propagation distance, with an additional unique ability of being electrically or chemi-

*Special Topic: Frontiers of Plasmonics (Ed. Hong-Xing Xu).

cally tunable [24, 32–34]. These extraordinary features of graphene plasmons have stimulated intense lines of investigation into both the fundamental properties of graphene plasmons [35–37] and potential applications in metamaterials [30, 38], modulators [39, 40], photodetectors [41], and sensors [42, 43]. Naturally, plasmon properties depend on the charge-carrier density, and high doping levels of graphene can be achieved either by electrostatic top-gating [44] or by chemical doping with surface treatment [45]. Despite the progress in achieving yet higher doping levels, pushing graphene plasmons to the near-infrared or even visible frequency regimes remains a challenge. In this paper, we review recent progress by emphasizing graphene plasmonics from fundamental light-matter interactions to some potential applications. The basic optical properties of nonradiating GPPs in an extended graphene sheet are first reviewed, and then three main subjects of graphene plasmonics are discussed: (i) excitation of graphene-plasmon polaritons, (ii) plasmon-phonon interactions in graphene on polar substrates, and (iii) tunable graphene plasmonics and its applications. Finally, we provide a brief outlook discussing challenges and perspectives of graphene plasmonics.

2 Fundamental properties of graphene

We begin with the electronic band structure of graphene calculated in the tight-binding approximation [47, 48], which is shown in Fig. 1(a). One of the unique properties of graphene is that the electron energy follows a linear dispersion relationship, $E(k) \approx \hbar v_{\mathrm{F}} k$, near the Dirac point, with Fermi energy $E_{\mathrm{F}} \approx \hbar v_{\mathrm{F}} \sqrt{\pi n}$, where $v_{\mathrm{F}} \approx 10^6\,\mathrm{m/s}$ is the Fermi velocity and n is the charge-carrier concentration. We note that, for pristine graphene in a nearest-neighbor tight-binding description, the unit cell is occupied by two electrons that at low temperatures fully populate the low-energy band [shown in blue in Fig. 1(a)], while the high-energy band (shown in red) remains empty. Thus, undoped graphene ($n = 0 \Rightarrow E_{\mathrm{F}} = 0$) behaves as a semimetal, sometimes also being referred to as a zero-bandgap semiconductor. The optical conductivity of pristine graphene, $\sigma = e^2/4\hbar$, is independent of any material parameters [49], giving a constant value of 2.3% for the optical absorption of single-layer graphene from the visible to near-infrared spectral windows. This featureless absorption is a manifestation of the massless Dirac fermions and quite remarkably the observed absorption ties closely with the fine-structure constant $\alpha = e^2/(4\pi\varepsilon_0\hbar c)$, i.e., $\pi\alpha \approx \pi/137 \approx 2.3\%$. Although it is already fascinating that an atomically thin layer can absorb as much as 2.3%, it is at least equally attractive that the optical properties of graphene can be substantially modified by changing the Fermi energy with the further addition of charge carriers [24, 32, 33].

Plasmons in graphene have many properties in common with longitudinal plasmon oscillations in two-dimensional electron gases supported by semiconductor heterostructures, but it is predicted that graphene also supports a transverse electric mode [50], which does not appear in the more common two-dimensional electron gases with parabolic energy dispersion. Here, we consider the transverse magnetic mode in an extended graphene sheet (characterized by its conductivity $\sigma(k_{//}, \omega)$, where $k_{//}$ is the wave vector of the GPP) sandwiched between two dielectric surroundings [see Fig. 1(b)]. The condition for the transverse magnetic polarized field propagating in the plane can be described as [35, 51]

$$\frac{\varepsilon^+}{\sqrt{k_{//}^2 - \frac{\varepsilon^+\omega^2}{c^2}}} + \frac{\varepsilon^-}{\sqrt{k_{//}^2 - \frac{\varepsilon^-\omega^2}{c^2}}} = \frac{\sigma(k_{//}, \omega)}{\mathrm{i}\varepsilon_0\omega}, \tag{1}$$

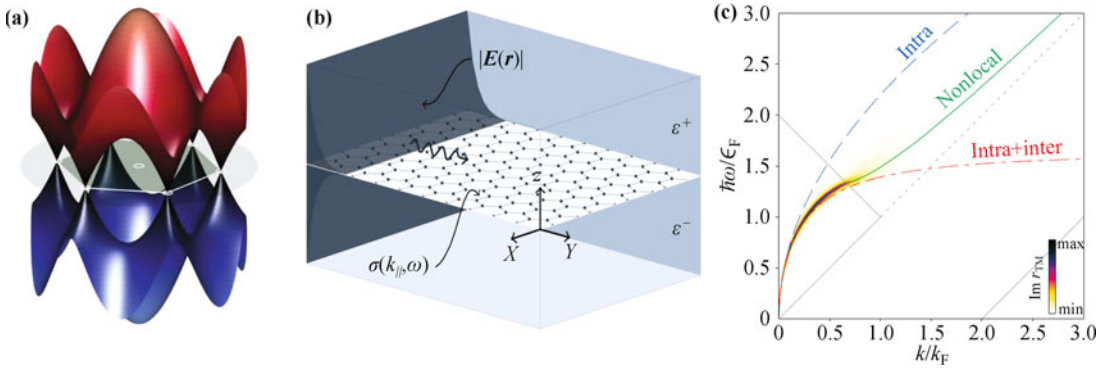

Fig. 1 **(a)** The dispersion relation of graphene's electrons within a tight-binding treatment. The first Brillouin zone is indicated in shaded green and delimited by white lines. **(b)** A graphene sheet, characterized by its conductivity $\sigma(k_{//}, \omega)$, sandwiched between super and substrates with relative dielectric functions $\varepsilon^{\pm}$. **(c)** Dispersion of GPPs in a free-standing graphene sheet ($\varepsilon^{\pm} = 1$) calculated with an analytical local-response intraband description (*the dashed blue line*), a full local-response conductivity (*the dashed-dotted line*) accounting for both intra and interband contributions, and finally the full nonlocal conductivity (*the green line*). Reproduced with permission from Ref. [46].

where ε_0 is the vacuum permittivity of free space and ε^+ and ε^- are the relative dielectric functions of the surrounding media. In the nonretarded regime where $k_{//} \gg \omega/c$, Eq. (1) can be simplified to

$$\omega = \frac{\sigma(k_{//},\omega)}{\mathrm{i}\varepsilon_0(\varepsilon^+ + \varepsilon^-)} k_{//}. \tag{2}$$

The optical conductivity $\sigma(k_{//},\omega)$ can be treated by using the nonlocal density-density response function [52, 53]. For the local-response limit, the conductivity $\sigma = \sigma_{\mathrm{inter}} + \sigma_{\mathrm{intra}}$ has distinct contributions from both interband and intraband transitions [35, 54]. In the low-temperature limit where the Fermi energy E_{F} exceeds the thermal energy, i.e., $E_{\mathrm{F}} \gg k_{\mathrm{B}}T$, the expressions are

$$\begin{aligned}\sigma_{\mathrm{intra}}(\omega) &= \frac{\mathrm{i}e^2 E_{\mathrm{F}}}{\pi\hbar^2(\omega + \mathrm{i}\gamma)},\\ \sigma_{\mathrm{inter}}(\omega) &= \frac{e^2}{4\hbar}\left[\theta(\hbar\omega - 2E_{\mathrm{F}}) + \frac{1}{\pi}\ln\left|\frac{2E_{\mathrm{F}} - \hbar\omega}{2E_{\mathrm{F}} + \hbar\omega}\right|\right],\end{aligned} \tag{3}$$

where γ is the relaxation rate and $\theta(x)$ is the Heaviside function. When considering the intraband transition solely, one obtains the following plasmon dispersion relation:

$$\begin{aligned}\omega &= \sqrt{\frac{e^2 E_{\mathrm{F}}}{\pi\hbar^2\varepsilon_0(\varepsilon^+ + \varepsilon^-)} k_{//}}\\ \Longleftrightarrow \frac{\hbar\omega}{E_{\mathrm{F}}} &= \sqrt{2\alpha\frac{c}{v_{\mathrm{F}}}\frac{2}{\varepsilon^+ + \varepsilon^-}\frac{k_{//}}{k_{\mathrm{F}}}}.\end{aligned} \tag{4}$$

This generic square-root dispersion relation is referred to as the local-response limit, because we have neglected the nonlocal response (spatial dispersion) in the derivation by treating the conductivity itself in the small-wave-vector limit, rather than maintaining the full-wave-vector dependence [55]. From the dimensionless form, we note that there is a "universal" dispersion relation irrespective of the particular doping level [see the dashed blue line in Fig. 1(c)].

In the zero-loss and zero-temperature limits, the dispersion of graphene surface-plasmon polaritons [see Fig. 1(c)] is obtained by three different models: the local-response intraband description, the full local-response conductivity, and the full nonlocal conductivity. Here, we have for the purpose of illustration considered typical numbers given by $E_{\mathrm{F}} = 0.4$ eV and $\hbar\gamma = 12$ meV.

3 Excitation of graphene-plasmon polaritons

To exploit and manipulate GPPs within various nanophotonic and optoelectronic applications, it is crucial to facilitate an efficient coupling of photons to GPPs for the development of future devices. Here, the nonradiating nature of GPPs is both a strength and a challenge. Graphene plasmons in nano- and micro-patterned graphene structures such as ribbons [41] and disks [60], so-called localized GPPs, can be easily excited. However, the strong spatial confinement of GPPs limits their applications when long propagation length is needed for, e.g., communication and information processing techniques. Here we pay special attention to propagating GPPs with the challenge to be excited by the mismatch of the wave vectors of the GPP and of light in vacuum. In this section, we review recently developed technologies and methods for the excitation of propagating GPPs.

Scattering-type scanning near-field optical microscopy (s-SNOM) was almost simultaneously proposed to detect and image propagating GPPs in two Nature papers published in the same issue [56, 61]. Chen *et al.* launched and detected propagating GPPs in tapered graphene nanostructures using an s-SNOM equipped with a metal-coated atomic-force microscopy (AFM) tip with infrared excitation light [see Fig. 2(a)]. In their setup, the metal-coated cantilever tip serves as an antenna, which converts the incident infrared light to GPPs with a wavelength of ~1/40 that in free space [see the middle plot in Fig. 2(a)]. Excited graphene plasmons are reflected at the ribbon edges, thus producing interference fringes recorded with the same AFM tip. Similarly, Fei *et al.* [61] worked with graphene on SiO_2 and excited GPPs using a slightly different incident wavelength compared to that used in Ref. [56], at which phonon excitation in SiO_2 is avoided [62]. The pattern of the calculated local density of optical states [see the bottom of Fig. 2(a)] matches quite well with the image for the GPP produced by s-SNOM. Both papers provide real-space imaging of GPPs with extremely high spatial resolution (~20 nm) limited only by the dimensions of the AFM probe. s-SNOM has been intensively used, e.g., for exploration of plasmons in graphene Moiré superlattices [63], for observation of ultraslow hyperbolic polariton propagation [64], and for observation of hyperbolic phonon-polaritons in boron nitride [65]. More recently, Alonso-González *et al.* [66] utilized an immovable metal gold rod standing on a graphene sheet as another kind of antenna. Near-field oscillation around the antenna was observed by using a pseudo-heterodyne interferometer and corroborates the existence of GPPs. Here, a normal Si tip was used, compared to its counterpart with a metal-coating layer [56, 61].

The butt-coupling technology widely used in nanophotonics is another way to couple light into GPPs. The coupling efficiency for the butt-coupling is mainly determined by the overlap of the modes. Owing to the extreme

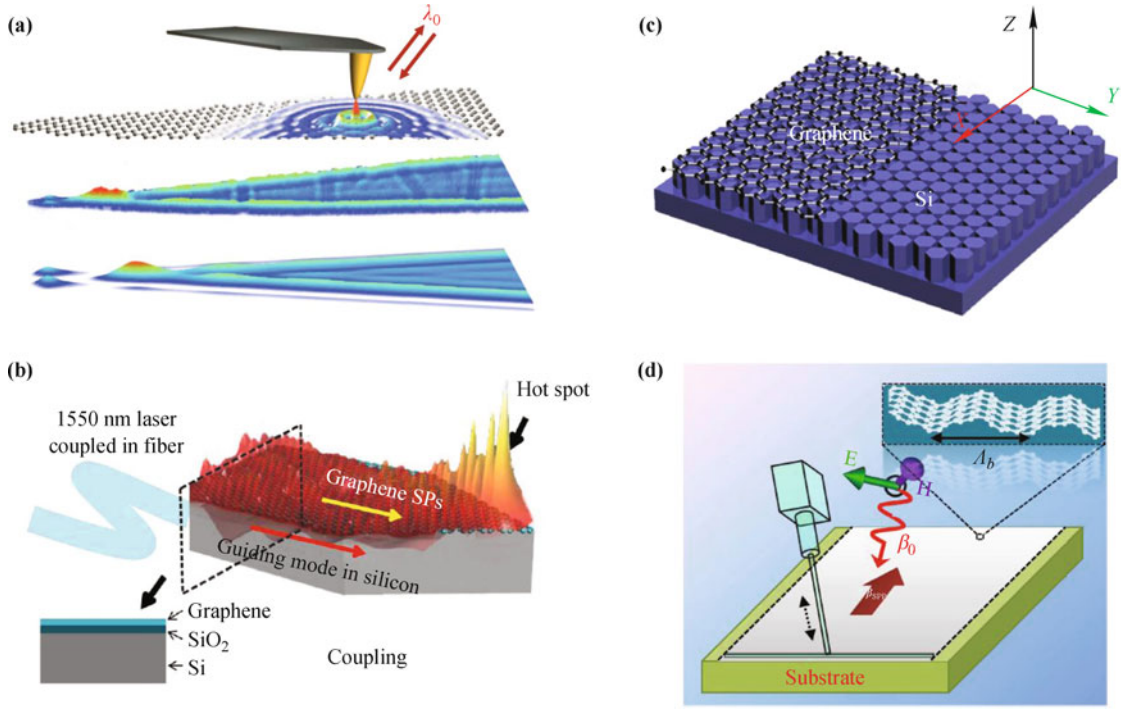

Fig. 2 **(a)** Excitation and detection of GPP by use of s-SNOM with a metal-coated tip (in yellow). From top to bottom: Schematic of experimental setup, near-field amplitude image, colour-scale image of the calculated local density of optical states. **(b)** Schematic of experimental configuration to excite GPP with the aid of the guiding mode in Si waveguide. The hot spot appearing at the tip position of the tapered geometry shows the characteristic of GPP. **(c)** Illustration of graphene covered nanopatterned Si substrate which provides a wavevector compensation for GPPs by grating coupling. **(d)** Geometry of 3D graphene grating driven by external acoustic stimulation. The inset shows a sinusoidal grating. Reproduced with permission from Ref. [56] (a), Ref. [57] (b), Ref. [58] (c), Ref. [59] (d).

mode confinement for GPPs, one really needs to suppress the size of the optical mode to achieve efficient coupling. Nikitin *et al.* [67] numerically proposed efficient coupling by the compression of surface polaritons on tapered bulk slabs of both polar and doped semiconductor materials. The infrared photons can be compressed from several micrometers to ∼200 nm, allowing the coupling of light to GPPs with ∼25% conversion efficiency. As shown in Fig. 2(b), Zhang *et al.* [57] used a guiding mode supported by a silicon waveguide to excite plasmons in graphene on top of silicon, where the graphene is doped by using the surface carrier transfer method with molybdenum trioxides. The observation of the hot spot in the tip [see Fig. 2(b)] by near-field scanning optical microscopy verifies the existence of GPPs in the near-infrared region.

In the plasmonics community, the grating coupler is widely used to compensate for the mismatch between the wave vector of plasmons in the metal and the wave vector of free-space radiation. A similar concept from plasmonic crystals was introduced to excite THz GPPs on a periodic hole array in a graphene sheet by Kitty *et al.* [68]. Zhu *et al.* [58] proposed using a two-dimensional subwavelength silicon grating beneath graphene to excite GPPs [see Fig. 2(c)]. With the aid of dielectric grating, transmission dips were observed by Fourier transform infrared spectroscopy (FTIR), indicating the existence and the excitation of GPPs in an extended graphene sheet. Along the same line, the excitation of GPPs by use of a one-dimensional silicon grating was also investigated theoretically [69] and experimentally [70]. Graphene is regarded as a perfect two-dimensional material. However, a three-dimensional graphene grating would be possible. By combining a proper substrate and applying acoustic mode excitation [see Fig. 2(d)], Farhat *et al.* [59] and Schiefele *et al.* [71] independently proposed exciting GPPs on curved graphene structures. More recent work on curved graphene geometries includes Refs. [72–75].

4 Plasmon-phonon interactions in graphene on a polar substrate

The electron mobility in a suspended single-layer graphene can be as high as 200 000 $cm^2 \cdot V^{-1} \cdot s^{-1}$. However, the carrier mobility drops significantly when graphene is placed on an insulating dielectric substrate such as SiO_2 [81]. The effects of polarizable substrates on carrier dynamics in graphene have been studied [82],

and one of the factors limiting the carrier mobility in graphene supported by a dielectric substrate is surface optical phonon scattering [83]. Owing to its weak phonon scattering, hexagonal boron nitride (h-BN) is believed to be a promising dielectric material for graphene [84] compared to other substrates such as SiO_2 and SiC. When the energy of plasmons becomes comparable with that of phonons, hybridization of plasmon and phonon modes occurs, leading to the breakdown of the Born–Oppenheimer approximation [85]. The interactions of plasmons with optical phonons in semiconductors have been studied [86]. In this section, we will review recent studies of plasmon-phonon coupling in graphene, including both theoretical investigations and experimental demonstrations.

In 2010, Hwang *et al.* calculated the collective excitation of coupled electron-phonon systems by taking into account the Coulomb coupling between electronic excitations in graphene and the optical phonon modes in the substrate [87]. The dispersion of the coupled plasmon-phonon modes shows that plasmon-phonon coupling is strong for all electron densities. By using the self-consistent linear response formalism, Jablan *et al.* predicted the existence of coupled plasmon-phonon excitations in graphene [76], which is shown in Fig. 3(a). The unique electron-phonon interaction in graphene results in unconventional mixing of plasmon and optical phonons, and the hybridization becomes stronger for larger doping values in graphene.

Strong phonon-plasmon coupled modes in graphene/SiC systems have been confirmed using angle-resolved reflection electron-energy-loss spectroscopy [77, 88], where graphene was prepared on a 6H-SiC crystalline wafer surface by solid-state graphitization [89]. Figure 3(b) shows the dispersion behavior of the loss peaks taken on graphene of various thicknesses. The dispersion looses its continuity both for one-monolayer graphene [the red dot in Fig. 3(b)] and two-monolayer graphene (the green squares), where crossovers occur between plasmons and surface optical phonons. The insert in Fig. 3(b) shows a schematic change of the dispersion curve where two modes couple with each other. s-SNOM was used to probe the mid-infrared plasmons in graphene [55, 61], and a similar technology was also explored to study plasmon-phonon interactions at the graphene-SiO_2 interface [62] [see Fig. 3(c)]. In that work, the beam of an infrared laser was focused on the metalized tip of an AFM cantilever. The strong near-field confinement

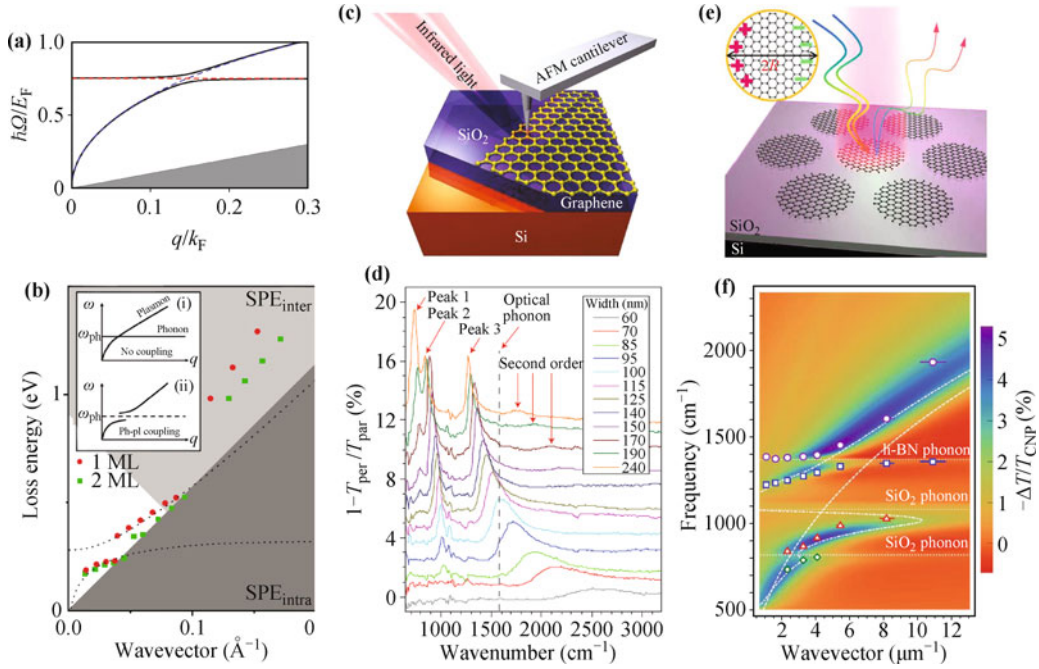

Fig. 3 **(a)** Dispersion of hybrid plasmon-phonon modes (*solid lines*) and of the uncoupled modes (*dashed lines*). Gray areas denote the region of single-particle damping. **(b)** The dispersion measured by angle-resolved reflection electron-energy-loss spectroscopy in single and multilayer graphene which couple strongly to surface optical phonon of SiC. **(c)** Schematics of the infrared nanoscopy (assisted by a nanoscale tip) to study Dirac plasmons at the graphene SiO_2 interface. **(d)** Extinction spectra of graphene ribbons on SiO_2 with different ribbon widths. **(e)** Schematics of mid-infrared reflection measurement by FTIR microscopy, where the inset shows the dipole oscillation in a graphene dot. **(f)** Hybridization of graphene plasmons and phonons in a monolayer h-BN sheet and SiO_2. Symbols represent experimental data, and the the dash-dot line indicates the calculated dispersion for graphene/SiO_2. Reproduced with permission from Ref. [76] (a), Ref. [77] (b), Ref. [62] (c), Ref. [78] (d), Ref. [79] (e), and Ref. [80] (f).

of mid-infrared radiation at the tip apex leads to high spatial resolution and high coupling that enables an investigation of the spectroscopic signature of plasmon-phonon interactions. The plasmon-phonon interaction and hybridization at the graphene-SiO_2 interface is observed by near-field nanoscopy.

Plasmon-phonon interactions in nanostructured graphene on SiO_2 substrate were also studied by using FTIR [78, 79]. Zhu *et al.* [79] demonstrated an effective approach for patterning graphene sheets into large-area ordered graphene nanostructures by combining nanosphere lithography with O_2 reactive ion etching, without having to use high-cost, low-throughput lithography or sophisticated instruments. Relying on nanosphere lithography technology, they have demonstrated stretch-tunable plasmonic structures, broadband enhancement of spontaneous emission, and high light-extraction enhancement [90–94]. A schematic of the FTIR mid-infrared reflection measurement scheme is illustrated in Fig. 3(e). This setup is used to probe the plasmon-phonon interactions in graphene. The hybridization of graphene plasmons and substrate phonons was experimentally demonstrated, showing coupling energies of the order of 20 meV. Extinction spectra for graphene nanoribbons are shown in Fig. 3(d), illustrating three main peaks [78]. The nanoribbons with dimensions as small as 60 nm were realized using electron-beam lithography. The multiple features shown in Fig. 3(d) are ascribed to plasmon-phonon coupled modes. More importantly, they provided a new damping mechanism for GPPs with the plasmon lifetime of 20 fs. The surface polar phonons in the SiO_2 substrate under graphene nanostructures not only modify the plasmon dispersion but also provide new channels for the damping of GPPs [78].

Experiments have also been extended to investigate the coupling between graphene plasmons and surface phonons in thin polar substrates [80, 95, 96]. The interactions between graphene plasmons and thin layers of poly(methyl methacrylate) (PMMA) were studied, showing that the PMMA phonon signature is strongly enhanced through graphene plasmon coupling [95]. Recent FTIR measurements [80, 96] verify the hybridization of graphene plasmons and phonons in a monolayer h-BN sheet. As an example [80], Fig. 3(f) illustrates the dispersion of graphene plasmons coupled with surface phonons, where experimental data are plotted as symbols. The three horizontal dotted lines indicate the optical phonon energies of h-BN and SiO_2, and the dashed-dotted line shows the coupled dispersion of graphene/SiO_2. In addition to the coupling between graphene plasmons and phonons from SiO_2, the interaction between graphene plasmons and phonons in h-BN sheet is also clearly observed, showing an avoided crossing (anticrossing) behavior near the h-BN optical phonon at 1370 cm^{-1}.

5 Tunable graphene plasmonics

Tunable plasmonic materials are essential in various areas of photonics, with applications ranging from perfect absorbers, high-technology frequency modulators and radiators to highly efficient chemical and biochemical sensing [24, 32, 41–43, 97–103]. Graphene supports plasmons that are tunable, providing a novel platform for tunable devices. The large mobility of charge carriers in graphene makes high-speed tunable plasmonics possible by electrical gating of graphene.

In 2011, Ju *et al.* reported plasmon excitations in graphene microribbons within the THz frequency range. As shown in Fig. 4(a), they demonstrated that graphene plasmon resonances can be tuned over a broad frequency range by changing the ribbon width and *in situ* backgating [41]. As in the studies of two-dimensional massless Dirac electrons, the graphene plasmon frequency also demonstrates a power-law characteristic behavior. In particular, the graphene plasmon resonances have remarkably large oscillator strengths, resulting in prominent room-temperature optical absorption peaks whereas plasmon absorption in a conventional two-dimensional electron gas was observed only at low temperature. Thus, graphene plasmons hold exceptional promise for optoelectronic applications by improving weak optical absorption at visible and infrared wavelengths. In 2013, Brar *et al.* demonstrated highly confined tunable mid-infrared plasmonics in graphene nanoresonators [97]. They mapped the wave-vector-dependent dispersion relations for graphene plasmons at mid-infrared energies from measurements of resonant frequency changes by tuning the charge-carrier density. In Fig. 4(b), we show an example where Fang *et al.* observed significantly enhanced graphene absorption (30%) in arrays of graphene nanodisks by using an $InIn_2O_3/BaF_2$ substrate and electron-beam lithography patterning [104]. By controlling the Fermi level of graphene (through a top-gated ion-gel), a wide range of plasmon tunability in the infrared was demonstrated in device geometries.

Dynamic control of thermal radiation through *in situ* modification of material emissivity could enable the design of novel infrared sources; however, the spectral characteristics of the radiated power are dictated by the electromagnetic energy density and emissivity, which are usually given by properties of the material at the particular temperature. Except for enhancing light absorption,

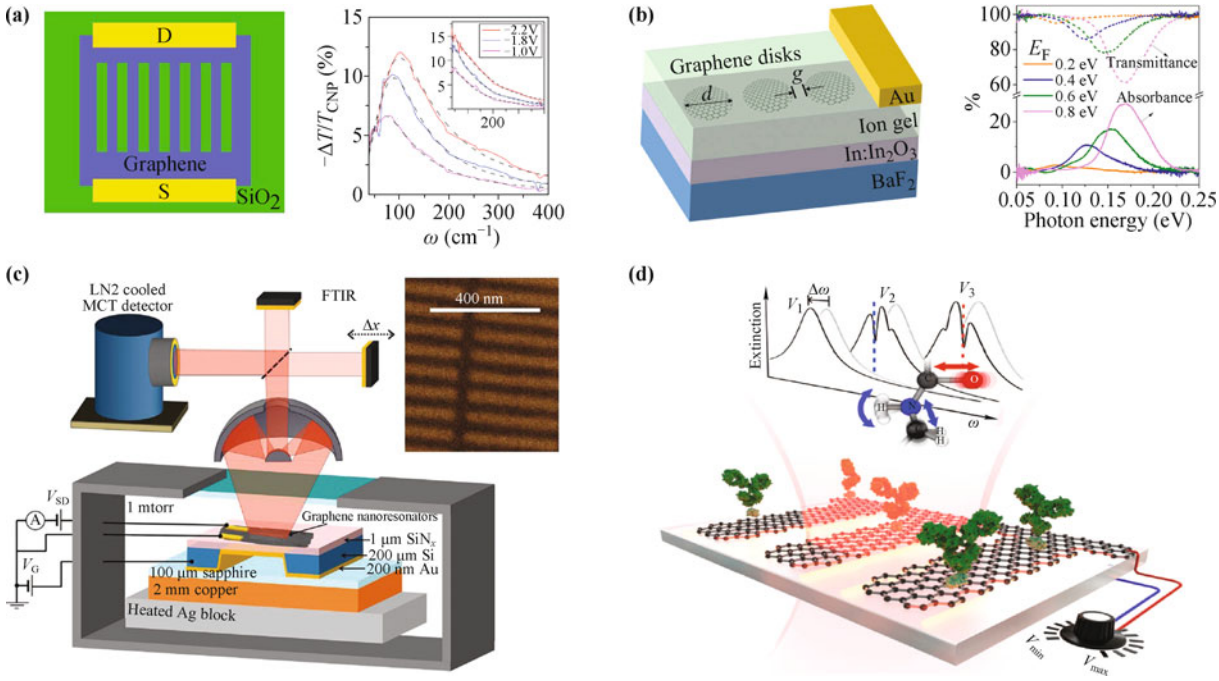

Fig. 4 **(a)** Graphene plasmonics for tunable terahertz metamaterials. Left: Illustration of electric back gating of the graphene micro-ribbons. Right: Control of terahertz plasmon excitations through electrical gating. **(b)** Active tunable absorption enhancement with graphene nanodisk arrays. Left: Scheme of the measured devices. Right: FTIR measurements for graphene nanodisk arrays with the tuning of Fermi level by electric top gating. **(c)** Set-up for electronic modulation of infrared radiation in graphene plasmonic resonators. Inset shows SEM image of the graphene structure. **(d)** Plasmonic biosensing with tunable graphene plasmonics implemented in the mid-infrared frequencies. Reproduced with permission from Ref. [41] (a), Ref. [104] (b), Ref. [105] (c), and Ref. [43] (d).

dynamic control of photon radiation could also be enabled by tunable graphene plasmonics. As shown by Brar *et al.* [Fig. 4(c)], the graphene resonators produced antenna-coupled black-body radiation, which manifested as narrow spectral emission peaks in the mid-infrared region [105]. Through continuously tuning of the nanoresonator charge-carrier density, the frequency and intensity of these spectral features can be modulated via electrostatic doping.

Biomaterials have abundant spectroscopic features (phonon vibration modes) in the mid-infrared frequencies [94]. However, these modes poorly interact with infrared light. By exploiting the unique electro-optical properties of GPPs, it is possible to realize a high-sensitivity graphene-based biosensor for chemically specific label-free detection of proteins. A mid-infrared GPP-based biosensor [see Fig. 4(d)] was reported by Rodrigo *et al.* [43]. The tunability of graphene allows selective probing of the protein at different frequencies. They showed superior sensitivity in the detection of their refractive index and vibrational fingerprints because of the high overlap between the strongly localized GPP mode and the nanometric biomolecules. In fact, from Eq. (4) it follows that the resonance wavelength shift $\Delta\lambda$ associated with a refractive-index change Δn, i.e., the refractometric sensitivity $\Delta\lambda/\Delta n$, is given by

$$\frac{\Delta\lambda}{\Delta n} \simeq f \times \frac{\lambda}{n}, \quad f = \frac{n^2}{n^2 + \varepsilon_s}, \tag{5}$$

where $\varepsilon^+ = n^2$, with n being the refractive index of the sensing medium above the graphene, and $\varepsilon^- = \varepsilon_s$ is the substrate dielectric function. Here, f quantifies the relative light overlap with the sensing medium in a similar fashion as has been introduced for dielectric refractive-index sensors based on, e.g., photonic crystals [106]. In the context of the sensing figure of merit, FOM $= (Q/\lambda)\,\Delta\lambda/\Delta n$ [107, 108], we thus get FOM $\simeq (\omega/\gamma)\,n/(n^2 + \varepsilon_s)$. Clearly, the prospects for low GPP damping will benefit sensors through an increased resonance quality factor $Q \simeq \omega/\gamma$.

Moreover, photocurrent in graphene can be harnessed by tunable intrinsic plasmons. Freitag *et al.* demonstrated polarization-sensitive and gate-tunable photodetection in graphene nanoribbon arrays [109]. The highly gate tunable graphene plasmon-phonon modes are longer lived and very promising for plasmonic enhanced photodetectors, with a life time exceeding an order of magnitude as compared with excitation of electron-hole pairs alone. The general principle of tunable graphene plasmons can open a new way to engineer photodetectors

from THz to infrared frequencies.

It is worth mentioning that the combination of graphene with traditional plasmonic structures or metamaterials could also provide the desired dielectric environment with an adjustable feature, resulting in high-speed tunable optical responses. In particular, interband and intraband transitions under optical excitation in graphene have been investigated. In the visible and near-infrared ranges, interband transitions result in a constant absorption of ∼2.3% by single-layer graphene at normal incidence and modulation of infrared absorption by electrically tuning its Fermi level; the absorption can be further improved by applying graphene in designed optical cavities [32, 110]. In the infrared and THz ranges, intraband transitions dominate, resulting in an optical conductivity well described by the Drude model [39]. Liang *et al.* demonstrated that a monolithically integrated graphene modulator can efficiently modulate the light intensity with a 100% modulation depth for a certain region of the pumping current at the THz range [40]. At infrared frequencies, electrical control of a plasmonic resonance using large-area graphene was demonstrated based on graphene-covered plasmonic nanowire [111] and metasurface systems [112], respectively. The combination of plasmonic structures with the possibility of controlling the Fermi level of graphene paves the way for advanced optoelectronic devices at optical frequencies.

6 Discussion and outlook

Graphene plasmons are commonly explored at mid-infrared and THz frequencies. To integrate graphene-plasmon concepts with existing more mature technologies, we need to extend plasmon frequencies into the telecommunication or visible-frequency windows. In graphene nanostructures, the plasmon-resonance frequency associated with localized graphene plasmons scales as $\sqrt{E_F/D}$ (with D being the characteristic dimension), which follows immediately from Eq. (4). Thus, higher frequencies can be achieved through both higher doping levels and/or reduced structure dimensions. Graphene plasmons were observed around 3.7 μm in graphene nanorings with a 20-nm width [104], i.e., with dimensions close to the limits of state-of-the-art electron-beam lithography. A natural way of pushing plasmons to even higher energies is to use bottom-up approaches, e.g., colloidal chemistry methods, or self-assembly of organic molecules [113–115]. As an example, Cai *et al.* presented their bottom-up approach to control the graphene nanoribbons with atomic resolution [113]. When the size of graphene structures becomes smaller and smaller, we eventually also need to be concerned with atomic-scale details, such as quantum mechanical effects associated with electronic edge states inevitably hosted by zigzag terminations of the graphene lattice [36, 37, 116], which shift and broaden the plasmon resonances.

It was predicted theoretically that graphene plasmons exhibit relatively long propagation distances. Experimentally, graphene plasmon losses are however still not fully up to this potential. s-SNOM [44] was used to estimate plasmon-propagation distances with the aid of interference fringes in the near vicinity of graphene edges, suggesting a relaxation time in graphene of 30 fs. Recently, relaxation times as large as 500 fs have been observed in high-quality graphene sandwiched between two films of h-BN [117]; this paves a promising path to the development of graphene nanophotonics and nano-optoelectronic devices. Wafer-scale single-crystalline graphene monolayers are considered an ideal platform for electronics and other applications. Single-crystalline graphene monolayer can be achieved by mechanical exfoliation [118, 119]; however, they are still only available with small areas. With the recent rapid development of chemical-vapor deposition, inch-sized single-crystalline graphene can be synthesized with a fast growth speed [120, 121]. Access to efficient production of wafer-scale monolayers may push graphene closer to real applications.

Finally, we note that here that we have only touched on the linear-response properties of graphene-plasmon polaritons; graphene may also host rich nonlinear dynamics [122–127].

Acknowledgements We thank Thomas Christensen and Nicolas Stenger for stimulating discussions. The Center for Nanostructured Graphene (CNG) is sponsored by the Danish National Research Foundation, Project DNRF103. We also acknowledge the Villum Foundation (341/300-123012) and the Danish Council for Independent Research (FNU 1323-00087).

References

1. S. A. Maier, Plasmonics: Fundamentals and Applications, New York: Springer, 2007
2. M. L. Brongersma, Introductory lecture: Nanoplasmonics, *Faraday Discuss.* 178, 9 (2015)

3. J. A. Schuller, E. S. Barnard, W. Cai, Y. C. Jun, J. S. White, and M. L. Brongersma, Plasmonics for extreme light concentration and manipulation, *Nat. Mater.* 9(3), 193 (2010)
4. Editorial, Focusing in on applications, *Nature Nanotechnol.* 10, 1 (2015)
5. A. Baev, P. N. Prasad, H. Ågren, M. Samoć, and M. Wegener, Metaphotonics: An emerging field with opportunities and challenges, *Phys. Rep.* 594, 1 (2015)
6. D. K. Gramotnev and S. I. Bozhevolnyi, Plasmonics beyond the diffraction limit, *Nat. Photonics* 4(2), 83 (2010)
7. D. K. Gramotnev and S. I. Bozhevolnyi, Nanofocusing of electromagnetic radiation, *Nat. Photonics* 8, 13 (2014)
8. S. Xiao and N. A. Mortensen, Surface-plasmon-polariton-induced suppressed transmission through ultrathin metal disk arrays, *Opt. Lett.* 36(1), 37 (2011)
9. S. Xiao, J. Zhang, L. Peng, C. Jeppesen, R. Malureanu, A. Kristensen, and N. A. Mortensen, Nearly zero transmission through periodically modulated ultrathin metal films, *Appl. Phys. Lett.* 97(7), 071116 (2010)
10. C. L. C. Smith, N. Stenger, A. Kristensen, N. A. Mortensen, and S. I. Bozhevolnyi, Gap and channeled plasmons in tapered grooves: A review, *Nanoscale* 7(21), 9355 (2015)
11. S. I. Bozhevolnyi, V. S. Volkov, E. Devaux, J. Y. Laluet, and T. W. Ebbesen, Channel plasmon subwavelength waveguide components including interferometers and ring resonators, *Nature* 440(7083), 508 (2006)
12. D. Ansell, I. P. Radko, Z. Han, F. J. Rodriguez, S. I. Bozhevolnyi, and A. N. Grigorenko, Hybrid graphene plasmonic waveguide modulators, *Nat. Commun.* 6, 8846 (2015)
13. S. Xiao, L. Liu, and M. Qiu, Resonator channel drop filters in a plasmon-polaritons metal, *Opt. Express* 14(7), 2932 (2006)
14. H. Xu, E. J. Bjerneld, M. Käll, and L. Börjesson, Spectroscopy of single hemoglobin molecules by surface enhanced Raman scattering, *Phys. Rev. Lett.* 83(21), 4357 (1999)
15. D. Punj, M. Mivelle, S. B. Moparthi, T. S. van Zanten, H. Rigneault, N. F. van Hulst, M. F. García-Parajó, and J. Wenger, A plasmonic "antenna-in-box" platform for enhanced single-molecule analysis at micromolar concentrations, *Nat. Nanotechnol.* 8(7), 512 (2013)
16. S. Kawata, Y. Inouye, and P. Verma, Plasmonics for near-field nano-imaging and superlensing, *Nat. Photonics* 3(7), 388 (2009)
17. F. Wei, D. Lu, H. Shen, W. Wan, J. L. Ponsetto, E. Huang, and Z. Liu, Wide field super-resolution surface imaging through plasmonic structured illumination microscopy, *Nano Lett.* 14(8), 4634 (2014)
18. H. A. Atwater and A. Polman, Plasmonics for improved photovoltaic devices, *Nat. Mater.* 9(3), 205 (2010)
19. S. Xiao, E. Stassen, and N. A. Mortensen, Ultrathinsilicon solar cells with enhanced photocurrentsassisted by plasmonic nanostructures, *J. Nanophot.* 6, 061503 (2012)
20. K. Kumar, H. Duan, R. S. Hegde, S. C. W. Koh, J. N. Wei, and J. K. W. Yang, Printing colour at the optical diffraction limit, *Nat. Nanotechnol.* 7(9), 557 (2012)
21. J. S. Clausen, E. Højlund-Nielsen, A. B. Christiansen, S. Yazdi, M. Grajower, H. Taha, U. Levy, A. Kristensen, and N. A. Mortensen, Plasmonic metasurfaces for coloration of plastic consumer products, *Nano Lett.* 14(8), 4499 (2014)
22. X. Zhu, C. Vannahme, E. Højlund-Nielsen, N. A. Mortensen, and A. Kristensen, Plasmonic colour laser printing, *Nat. Nanotechnol.* doi:10.1038/nnano.2015.285 (2016)
23. J. N. Anker, W. P. Hall, O. Lyandres, N. C. Shah, J. Zhao, and R. P. Van Duyne, Biosensing with plasmonic nanosensors, *Nat. Mater.* 7(6), 442 (2008)
24. M. Liu, X. Yin, E. Ulin-Avila, B. Geng, T. Zentgraf, L. Ju, F. Wang, and X. Zhang, A graphene-based broadband optical modulator, *Nature* 474(7349), 64 (2011)
25. A. C. Ferrari, F. Bonaccorso, V. Fal'ko, K. S. Novoselov, S. Roche, et al., Science and technology roadmap for graphene, related two-dimensional crystals, and hybrid systems, *Nanoscale* 7(11), 4598 (2015)
26. A. N. Grigorenko, M. Polini, and K. S. Novoselov, Graphene plasmonics, *Nat. Photonics* 6, 749 (2012)
27. Y. V. Bludov, A. Ferreira, N. M. R. Peres, and M. I. Vasilevskiy, A primer on surface plasmon-polaritons in graphene, *Int. J. Mod. Phys. B* 27(10), 1341001 (2013)
28. F. J. García de Abajo, Graphene plasmonics: Challenges and opportunities, *ACS Photonics* 1(3), 135 (2014)
29. T. Low and P. Avouris, Graphene plasmonics for terahertz to mid-infrared applications, *ACS Nano* 8(2), 1086 (2014)
30. A. Vakil and N. Engheta, Transformation optics using graphene, *Science* 332(6035), 1291 (2011)
31. H. Raether, Surface Plasmons on Smooth and Rough Surfaces on Gratings, Berlin: Springer, 1988
32. Y. Ding, X. Zhu, S. Xiao, H. Hu, L. H. Frandsen, N. A. Mortensen, and K. Yvind, Effective electro-optical modulation with high extinction ratio by a graphene-silicon microring resonator, *Nano Lett.* 15(7), 4393 (2015)
33. C. T. Phare, Y.-H. D. Lee, J. Cardenas, and M. Lipson, Graphene electro-optic modulator with 30 GHz bandwidth, *Nat. Photonics* 9, 511 (2015)
34. I. Goykhman, U. Sassi, B. Desiatov, N. Mazurski, S. Milana, D. de Fazio, A. Eiden, J. Khurgin, J. Shappir, U. Levy, and A. C. Ferrari, On-chip integrated, silicon-graphene plasmonic Schottky photodetector, with high responsivity and avalanche photogain, arXiv: 1512.08153
35. F. H. Koppens, D. E. Chang, and F. J. García de Abajo, Graphene plasmonics: A platform for strong light-matter interactions, *Nano Lett.* 11(8), 3370 (2011)
36. S. Thongrattanasiri, A. Manjavacas, and F. J. García de Abajo, Quantum finite-size effects in graphene plasmons, *ACS Nano* 6(2), 1766 (2012)
37. T. Christensen, W. Wang, A.-P. Jauho, M. Wubs, and N. A. Mortensen, Classical and quantum plasmonics in graphene nanodisks: The role of edge states, *Phys. Rev. B* 90, 241414(R) (2014)

38. S. H. Lee, M. Choi, T. T. Kim, S. Lee, M. Liu, X. Yin, H. K. Choi, S. S. Lee, C. G. Choi, S. Y. Choi, X. Zhang, and B. Min, Switching terahertz waves with gate-controlled active graphene metamaterials, *Nat. Mater.* 11(11), 936 (2012)
39. B. Sensale-Rodriguez, R. Yan, M. M. Kelly, T. Fang, K. Tahy, W. S. Hwang, D. Jena, L. Liu, and H. G. Xing, Broadband graphene terahertz modulators enabled by intraband transitions, *Nat. Commun.* 3, 780 (2012)
40. G. Liang, X. Hu, X. Yu, Y. Shen, L. H. Li, A. G. Davies, E. H. Linfield, H. K. Liang, Y. Zhang, S. F. Yu, and Q. J. Wang, Integrated terahertz graphene modulator with 100% modulation depth, *ACS Photonics* 2(11), 1559 (2015)
41. L. Ju, B. Geng, J. Horng, C. Girit, M. Martin, Z. Hao, H. A. Bechtel, X. Liang, A. Zettl, Y. R. Shen, and F. Wang, Graphene plasmonics for tunable terahertz metamaterials, *Nat. Nanotechnol.* 6(10), 630 (2011)
42. A. Marini, I. Silveiro, and F. J. García de Abajo, Molecular sensing with tunable graphene plasmons, *ACS Photonics* 2(7), 876 (2015)
43. D. Rodrigo, O. Limaj, D. Janner, D. Etezadi, F. J. García de Abajo, V. Pruneri, and H. Altug, Mid-infrared plasmonic biosensing with graphene, *Science* 349(6244), 165 (2015)
44. C. F. Chen, C. H. Park, B. W. Boudouris, J. Horng, B. Geng, C. Girit, A. Zettl, M. F. Crommie, R. A. Segalman, S. G. Louie, and F. Wang, Controlling inelastic light scattering quantum pathways in graphene, *Nature* 471(7340), 617 (2011)
45. I. Khrapach, F. Withers, T. H. Bointon, D. K. Polyushkin, W. L. Barnes, S. Russo, and M. F. Craciun, Novel highly conductive and transparent graphene-based conductors, *Adv. Mater.* 24(21), 2844 (2012)
46. T. Christensen, From classical to quantum plasmonics in three and two dimensions, PhD Thesis, Technical University of Denmark, 2015
47. A. Bostwick, T. Ohta, T. Seyller, K. Horn, and E. Rotenberg, Quasiparticle dynamics in graphene, *Nat. Phys.* 3(1), 36 (2007)
48. A. H. Castro Neto, F. Guinea, N. M. R. Peres, K. S. Novoselov, and A. K. Geim, The electronic properties of graphene, *Rev. Mod. Phys.* 81(1), 109 (2009)
49. R. R. Nair, P. Blake, A. N. Grigorenko, K. S. Novoselov, T. J. Booth, T. Stauber, N. M. R. Peres, and A. K. Geim, Fine structure constant defines visual transparency of graphene, *Science* 320(5881), 1308 (2008)
50. S. A. Mikhailov and K. Ziegler, New electromagnetic mode in graphene, *Phys. Rev. Lett.* 99(1), 016803 (2007)
51. M. Jablan, H. Buljan, and M. Soljačić, Plasmonics in graphene at infrared frequencies, *Phys. Rev. B* 80(24), 245435 (2009)
52. B. Wunsch, T. Stauber, F. Sols, and F. Guinea, Dynamical polarization of graphene at finite doping, *New J. Phys.* 8(12), 318 (2006)
53. E. H. Hwang and S. Das Sarma, Dielectric function, screening, and plasmons in two-dimensional graphene, *Phys. Rev. B* 75(20), 205418 (2007)
54. L. A. Falkovsky and A. A. Varlamov, Space-time dispersion of graphene conductivity, *Eur. Phys. J. B* 56(4), 281 (2007)
55. S. Raza, S. I. Bozhevolnyi, M. Wubs, and N. A. Mortensen, Nonlocal optical response in metallic nanostructures, *J. Phys.: Condens. Matter* 27(18), 183204 (2015)
56. J. Chen, M. Badioli, P. Alonso-González, S. Thongrattanasiri, F. Huth, J. Osmond, M. Spasenović, A. Centeno, A. Pesquera, P. Godignon, A. Z. Elorza, N. Camara, F. J. García de Abajo, R. Hillenbrand, and F. H. L. Koppens, Optical nano-imaging of gate-tunable graphene plasmons, *Nature* 487(7405), 77 (2012)
57. Q. Zhang, X. Li, M. M. Hossain, Y. Xue, J. Zhang, J. Song, J. Liu, M. D. Turner, S. Fan, Q. Bao, and M. Gu, Graphene surface plasmons at the near-infrared optical regime, *Sci. Rep.* 4, 6559 (2014)
58. X. Zhu, W. Yan, P. U. Jepsen, O. Hansen, N. A. Mortensen, and S. Xiao, Experimental observation of plasmons in a graphene monolayer resting on a two-dimensional subwavelength silicon grating, *Appl. Phys. Lett.* 102(13), 131101 (2013)
59. M. Farhat, S. Guenneau, and H. Bağcı, Exciting graphene surface plasmon polaritons through light and sound interplay, *Phys. Rev. Lett.* 111(23), 237404 (2013)
60. H. Yan, X. Li, B. Chandra, G. Tulevski, Y. Wu, M. Freitag, W. Zhu, P. Avouris, and F. Xia, Tunable infrared plasmonic devices using graphene/insulator stacks, *Nat. Nanotechnol.* 7(5), 330 (2012)
61. Z. Fei, A. S. Rodin, G. O. Andreev, W. Bao, A. S. McLeod, M. Wagner, L. M. Zhang, Z. Zhao, M. Thiemens, G. Dominguez, M. M. Fogler, A. H. Castro Neto, C. N. Lau, F. Keilmann, and D. N. Basov, Gate-tuning of graphene plasmons revealed by infrared nano-imaging, *Nature* 487(7405), 82 (2012)
62. Z. Fei, G. O. Andreev, W. Bao, L. M. Zhang, A. S. McLeod, C. Wang, M. K. Stewart, Z. Zhao, G. Dominguez, M. Thiemens, M. M. Fogler, M. J. Tauber, A. H. Castro-Neto, C. N. Lau, F. Keilmann, and D. N. Basov, Infrared nanoscopy of Dirac plasmons at the graphene-SiO_2 interface, *Nano Lett.* 11(11), 4701 (2011)
63. G. X. Ni, H. Wang, J. S. Wu, Z. Fei, M. D. Goldflam, F. Keilmann, B. Özyilmaz, A. H. Castro Neto, X. M. Xie, M. M. Fogler, and D. N. Basov, Plasmons in graphene Moiré superlattices, *Nat. Mater.* 14(12), 1217 (2015)
64. E. Yoxall, M. Schnell, A. Y. Nikitin, O. Txoperena, A. Woessner, M. B. Lundeberg, F. Casanova, L. E. Hueso, F. H. L. Koppens, and R. Hillenbrand, Direct observation of ultraslow hyperbolic polariton propagation with negative phase velocity, *Nat. Photonics* 9(10), 674 (2015)
65. P. Li, M. Lewin, A. V. Kretinin, J. D. Caldwell, K. S. Novoselov, T. Taniguchi, K. Watanabe, F. Gaussmann, and T. Taubner, Hyperbolic phonon-polaritons in boron nitride

for near-field optical imaging and focusing, *Nat. Commun.* 6, 7507 (2015)

66. P. Alonso-González, A. Y. Nikitin, F. Golmar, A. Centeno, A. Pesquera, S. Vélez, J. Chen, G. Navickaite, F. Koppens, A. Zurutuza, F. Casanova, L. E. Hueso, and R. Hillenbrand, Controlling graphene plasmons with resonant metal antennas and spatial conductivity patterns, *Science* 344(6190), 1369 (2014)
67. A. Y. Nikitin, P. Alonso-González, and R. Hillenbrand, Efficient coupling of light to graphene plasmons by compressing surface polaritons with tapered bulk materials, *Nano Lett.* 14(5), 2896 (2014)
68. K. Y. M. Yeung, J. Chee, H. Yoon, Y. Song, J. Kong, and D. Ham, Far-infrared graphene plasmonic crystals for plasmonic band engineering, *Nano Lett.* 14(5), 2479 (2014)
69. W. Gao, J. Shu, C. Qiu, and Q. Xu, Excitation of plasmonic waves in graphene by guided-mode resonances, *ACS Nano* 6(9), 7806 (2012)
70. W. Gao, G. Shi, Z. Jin, J. Shu, Q. Zhang, R. Vajtai, P. M. Ajayan, J. Kono, and Q. Xu, Excitation and active control of propagating surface plasmon polaritons in graphene, *Nano Lett.* 13(8), 3698 (2013)
71. J. Schiefele, J. Pedrós, F. Sols, F. Calle, and F. Guinea, Coupling light into graphene plasmons through surface acoustic waves, *Phys. Rev. Lett.* 111(23), 237405 (2013)
72. T. Christensen, A. P. Jauho, M. Wubs, and N. A. Mortensen, Localized plasmons in graphene-coated nanospheres, *Phys. Rev. B* 91(12), 125414 (2015)
73. W. Wang, B. Li, E. Stassen, N. A. Mortensen, and J. Christensen, Localized surface plasmons in vibrating graphene nanodisks, *Nanoscale*, 2016, DOI: 10.1039/C5NR08812G, arXiv: 1502.00535
74. A. Reserbat-Plantey, K. G. Schädler, L. Gaudreau, G. Navickaite, J. Güttinger, D. Chang, C. Toninelli, A. Bachtold, and F. H. L. Koppens, Electromechanical control of nitrogen-vacancy defect emission using graphene NEMS, *Nat. Commun.* 7, 10218 (2016)
75. D. Smirnova, S. H. Mousavi, Z. Wang, Y. S. Kivshar, and A. B. Khanikaev, Trapping and guiding surface plasmons in curved graphene landscapes, arXiv: 1508.02729
76. M. Jablan, M. Soljačić, and H. Buljan, Unconventional plasmon-phonon coupling in graphene, *Phys. Rev. B* 83(16), 161409 (2011)
77. Y. Liu and R. F. Willis, Plasmon-phonon strongly coupled mode in epitaxial graphene, *Phys. Rev. B* 81(8), 081406 (2010)
78. H. Yan, T. Low, W. Zhu, Y. Wu, M. Freitag, X. Li, F. Guinea, P. Avouris, and F. Xia, Damping pathways of mid-infrared plasmons in graphene nanostructures, *Nat. Photonics* 7(5), 394 (2013)
79. X. Zhu, W. Wang, W. Yan, M. B. Larsen, P. Bøggild, T. G. Pedersen, S. Xiao, J. Zi, and N. A. Mortensen, Plasmon-phonon coupling in large-area graphene dot and antidot arrays fabricated by nanosphere lithography, *Nano Lett.* 14(5), 2907 (2014)
80. V. W. Brar, M. S. Jang, M. Sherrott, S. Kim, J. J. Lopez, L. B. Kim, M. Choi, and H. Atwater, Hybrid surface-phonon-plasmon polariton modes in graphene/monolayer h-BN heterostructures, *Nano Lett.* 14(7), 3876 (2014)
81. K. Bolotin, K .Sikes, Z. Jiang, M. Klima, G. Fudenberg, J. Hone, P. Kim, and H. Stormer, Ultrahigh electron mobility in suspended graphene, *Solid State Commun.* 146(9–10), 351 (2008)
82. S. Fratini and F. Guinea, Substrate-limited electron dynamics in graphene, *Phys. Rev. B* 77(19), 195415 (2008)
83. K. Hess and P. Vogl, Remote polar phonon scattering in silicon inversion layers, *Solid State Commun.* 30(12), 807 (1979)
84. C. R. Dean, A. F. Young, I. Meric, C. Lee, L. Wang, S. Sorgenfrei, K. Watanabe, T. Taniguchi, P. Kim, K. L. Shepard, and J. Hone, Boron nitride substrates for high-quality graphene electronics, *Nat. Nanotechnol.* 5(10), 722 (2010)
85. S. Pisana, M. Lazzeri, C. Casiraghi, K. S. Novoselov, A. K. Geim, A. C. Ferrari, and F. Mauri, Breakdown of the adiabatic Born-Oppenheimer approximation in graphene, *Nat. Mater.* 6(3), 198 (2007)
86. A. Mooradian and G. B. Wright, Observation of the interaction of plasmons with longitudinal optical phonons in GaAs, *Phys. Rev. Lett.* 16(22), 999 (1966)
87. E. H. Hwang, R. Sensarma, and S. Das Sarma, Plasmon-phonon coupling in graphene, *Phys. Rev. B*82(19), 195406 (2010)
88. R. J. Koch, T. Seyller, and J. A. Schaefer, Strong phonon-plasmon coupled modes in the graphene/silicon carbide heterosystem, *Phys. Rev. B* 82(20), 201413 (2010)
89. I. Forbeaux, J. M. Themlin, and J. M. Debever, Heteroepitaxial graphite on 6H-SiC(0001): Interface formation through conduction-band electronic structure, *Phys. Rev. B* 58(24), 16396 (1998)
90. Y. Ou, X. Zhu, V. Jokubavicius, R. Yakimova, N. A. Mortensen, M. Syväjärvi, S. Xiao, and H. Ou, Broadband antireflection and light extraction enhancement in fluorescent SiC with nanodome structures, *Sci. Rep.* 4, 4662 (2014)
91. X. Zhu, Y. Ou, V. Jokubavicius, M. Syvajarvi, O. Hansen, H. Ou, N. A. Mortensen, and S. Xiao, Broadband light-extraction enhanced by arrays of whispering gallery resonators, *Appl. Phys. Lett.* 101(24), 241108 (2012)
92. X. Zhu, C. Zhang, X. Liu, O. Hansen, S. Xiao, N. A. Mortensen, and J. Zi, Evaporation of water droplets on "lock-and-key" structures with nanoscale features, *Langmuir* 28(25), 9201 (2012)
93. X. Zhu, F. Xie, L. Shi, X. Liu, N. A. Mortensen, S. Xiao, J. Zi, and W. Choy, Broadband enhancement of spontaneous emission in a photonic-plasmonic structure, *Opt. Lett.* 37(11), 2037 (2012)
94. X. Zhu, S. Xiao, L. Shi, X. Liu, J. Zi, O. Hansen, and N. A. Mortensen, A stretch-tunable plasmonic structure with a

polarization-dependent response, *Opt. Express* 20(5), 5237 (2012)

95. Y. Li, H. Yan, D. B. Farmer, X. Meng, W. Zhu, R. M. Osgood, T. F. Heinz, and P. Avouris, Graphene plasmon enhanced vibrational sensing of surface-adsorbed layers, *Nano Lett.* 14(3), 1573 (2014)
96. I. D. Barcelos, A. R. Cadore, L. C. Campos, A. Malachias, K. Watanabe, T. Taniguchi, F. C. Maia, R. Freitas, and C. Deneke, Graphene/h-BN plasmon-phonon coupling and plasmon delocalization observed by infrared nanospectroscopy, *Nanoscale* 7(27), 11620 (2015)
97. V. W. Brar, M. S. Jang, M. Sherrott, J. J. Lopez, and H. A. Atwater, Highly confined tunable mid-infrared plasmonics in graphene nanoresonators, *Nano Lett.* 13(6), 2541 (2013)
98. M. M. Jadidi, A. B. Sushkov, R. L. Myers-Ward, A. K. Boyd, K. M. Daniels, D. K. Gaskill, M. S. Fuhrer, H. D. Drew, and T. E. Murphy, Tunable terahertz hybrid metal-graphene plasmons, *Nano Lett.* 15(10), 7099 (2015)
99. M. K. Hedayati, A. U. Zillohu, T. Strunskus, F. Faupel, and M. Elbahri, Plasmonic tunable metamaterial absorber as ultraviolet protection film, *Appl. Phys. Lett.* 104(4), 041103 (2014)
100. D. Franklin, Y. Chen, A.Vazquez-Guardado, S. Modak, J. Boroumand, D. Xu, S. T. Wu, and D. Chanda, Polarization-independent actively tunable colour generation on imprinted plasmonic surfaces, *Nat. Commun.* 6, 7337 (2015)
101. A. Yang, T. B. Hoang, M. Dridi, C. Deeb, M. H. Mikkelsen, G. C. Schatz, and T. W. Odom, Real-time tunable lasing from plasmonic nanocavity arrays, *Nat. Commun.* 6, 6939 (2015)
102. G. C. Dyer, G. R. Aizin, S. J. Allen, A. D. Grine, D. Bethke, J. L. Reno, and E. A. Shaner, Induced transparency by coupling of Tamm and defect states in tunable terahertz plasmonic crystals, *Nat. Photonics* 7(11), 925 (2013)
103. B. Fluegel, A. Mascarenhas, D. W. Snoke, L. N. Pfeiffer, and K. West, Plasmonic all-optical tunable wavelength shifter, *Nat. Photonics* 1(12), 701 (2007)
104. Z. Fang, S. Thongrattanasiri, A. Schlather, Z. Liu, L. Ma, Y. Wang, P. M. Ajayan, P. Nordlander, N. J. Halas, and F. J. García de Abajo, Gated tunability and hybridization of localized plasmons in nanostructured graphene, *ACS Nano* 7(3), 2388 (2013)
105. V. W. Brar, M. C. Sherrott, M. S. Jang, S. Kim, L. Kim, M. Choi, L. A. Sweatlock, and H. A. Atwater, Electronic modulation of infrared radiation in graphene plasmonic resonators, *Nat. Commun.* 6, 7032 (2015)
106. N. A. Mortensen, S. Xiao, and J. Pedersen, Liquid-infiltrated photonic crystals: Enhanced light-matter interactions for lab-on-a-chip applications, *Microfluid. Nanofluidics* 4(1), 117 (2008)
107. L. J. Sherry, R. Jin, C. A. Mirkin, G. C. Schatz, and R. P. Van Duyne, Localized surface plasmon resonance spectroscopy of single silver triangular nanoprisms, *Nano Lett.* 6(9), 2060 (2006)
108. C. Jeppesen, S. Xiao, N. A. Mortensen, and A. Kristensen, Metamaterial localized resonance sensors: Prospects and limitations, *Opt. Express* 18(24), 25075 (2010)
109. M. Freitag, T. Low, W. Zhu, H. Yan, F. Xia, and P. Avouris, Photocurrent in graphene harnessed by tunable intrinsic plasmons, *Nat. Commun.* 4, 1951 (2013)
110. X. Zhu, L. Shi, M. S. Schmidt, A. Boisen, O. Hansen, J. Zi, S. Xiao, and N. A. Mortensen, Enhanced light-matter interactions in graphene-covered gold nanovoid arrays, *Nano Lett.* 13(10), 4690 (2013)
111. J. Kim, H. Son, D. J. Cho, B. Geng, W. Regan, S. Shi, K. Kim, A. Zettl, Y. R. Shen, and F. Wang, Electrical control of optical plasmon resonance with graphene, *Nano Lett.* 12(11), 5598 (2012)
112. S. H. Mousavi, I. Kholmanov, K. B. Alici, D. Purtseladze, N. Arju, K. Tatar, D. Y. Fozdar, J. W. Suk, Y. Hao, A. B. Khanikaev, R. S. Ruoff, and G. Shvets, Inductive tuning of Fano-resonant metasurfaces using plasmonic response of graphene in the mid-infrared, *Nano Lett.* 13(3), 1111 (2013)
113. J. Cai, P. Ruffieux, R. Jaafar, M. Bieri, T. Braun, S. Blankenburg, M. Muoth, A. P. Seitsonen, M. Saleh, X. Feng, K. Müllen, and R. Fasel, Atomically precise bottom-up fabrication of graphene nanoribbons, *Nature* 466(7305), 470 (2010)
114. X. Li, X. Wang, L. Zhang, S. Lee, and H. Dai, Chemically derived, ultrasmooth graphene nanoribbon semiconductors, *Science* 319(5867), 1229 (2008)
115. S. Rasappa, J. M. Caridad, L. Schulte, A. Cagliani, D. Borah, M. A. Morris, P. Bøggild, and S. Ndoni, High quality sub-10 nm graphene nanoribbons by on-chip PS-b-PDMS block copolymer lithography, *RSC Adv.* 5, 66711 (2015)
116. W. Wang, T. Christensen, A. P. Jauho, K. S. Thygesen, M. Wubs, and N. A. Mortensen, Plasmonic eigenmodes in individual and bow-tie graphene nanotriangles, *Sci. Rep.* 5, 9535 (2015)
117. A. Woessner, M. B. Lundeberg, Y. Gao, A. Principi, P. Alonso-González, M. Carrega, K.Watanabe, T. Taniguchi, G. Vignale, M. Polini, J. Hone, R. Hillenbrand, and F. H. L. Koppens, Highly confined low-loss plasmons in graphene-boron nitride heterostructures, *Nat. Mater.* 14(4), 421 (2015)
118. K. S. Novoselov, A. K. Geim, S. V. Morozov, D. Jiang, Y. Zhang, S. V. Dubonos, I. V. Grigorieva, and A. A. Firsov, Electric field effect in atomically thin carbon films, *Science* 306, 666 (2004)
119. Y. Zhang, Y. W. Tan, H. L. Stormer, and P. Kim, Experimental observation of the quantum Hall effect and Berry's phase in graphene, *Nature* 438(7065), 201 (2005)
120. Y. Hao, M. S. Bharathi, L. Wang, Y. Liu, H. Chen, S. Nie, X. Wang, H. Chou, C. Tan, B. Fallahazad, H. Ramanarayan, C. W. Magnuson, E. Tutuc, B. I. Yakobson, K. F. McCarty, Y. W. Zhang, P. Kim, J. Hone, L. Colombo, and R. S. Ruoff, The role of surface oxygen in the growth of large single-crystal graphene on copper, *Science* 342(6159), 720 (2013)

121. T. Wu, X. Zhang, Q. Yuan, J. Xue, G. Lu, Z. Liu, H. Wang, H. Wang, F. Ding, Q. Yu, X. Xie, and M. Jiang, Fast growth of inch-sized single-crystalline graphene from a controlled single nucleus on Cu-Ni alloys, *Nat. Mater.* 15(1), 43 (2016)

122. J. L. Cheng, N. Vermeulen, and J. E. Sipe, Third order optical nonlinearity of graphene, *New J. Phys.* 16(5), 053014 (2014)

123. N. M. R. Peres, Y. V. Bludov, J. E. Santos, A. P. Jauho, and M. I. Vasilevskiy, Optical bistability of graphene in the terahertz range, *Phys. Rev. B* 90(12), 125425 (2014)

124. D. A. Smirnova, I. V. Shadrivov, A. E. Miroshnichenko, A. I. Smirnov, and Y. S. Kivshar, Second-harmonic generation by a graphene nanoparticle, *Phys. Rev. B* 90(3), 035412 (2014)

125. T. Christensen, W. Yan, A.-P.Jauho, M. Wubs, and N. A. Mortensen, Kerr nonlinearity and plasmonic bistability in graphene nanoribbons, *Phys. Rev. B* 92, 121407(R) (2015)

126. J. D. Cox and F. Javier García de Abajo, Electrically tunable nonlinear plasmonics in graphene nanoislands, *Nat. Commun.* 5, 5725 (2014)

127. J. D. Cox and F. J. García de Abajo, Plasmon-enhanced nonlinear wave mixing in nanostructured graphene, *ACS Photonics* 2(2), 306 (2015)